ISSN: 2756-2638
Transactions on Engineering and Computing Sciences; Vol. 14 No. 01 (2026) (17-31)
https://doi.org/10.14738/tmlai.1401.19868

Tail Design for Improved Stability and Control of a Short Take Off and Landing Aircraft at High Angles of Attack

Olanrewaju Miracle Oyewola*, Alex Armstrong, Roger Jaramilo, Matthew Johnson and Thomas MacDonald

1. Department of Mechanical Engineering, University of Alaska Fairbanks, Alaska, USA

Abstract: Short takeoff and landing (STOL) aircraft are an important part of life in Alaska. These aircraft allow pilots to land in places that would otherwise be considered too small for a standard aircraft. Part of being a STOL capable aircraft requires slow speed flight at high angles of attack. Many of the true STOL aircraft in Alaska are modified commercially available aircraft that were never designed for these high angles of attack. This paper will propose and analyze a set of modifications to an already modified Piper Cub to improve the tail authority at these higher angles of attack. These modifications include changing the cross-sectional geometry of the horizontal stabilizer, increasing the area of the tail, and increasing the length of the wing leading edge slats to improve flow quality. CFD was performed on both the original and modified designs in a variety of flight configurations to evaluate the stability and control of the aircraft system at a free stream velocity of 30mph. Analysis of the CFD found that the elevator authority increases by 12.3% and the maximum achievable angle of attack increases by approximately 5.5 degrees.

Keywords: Tail design, Short Take Off and Landing, Stability and Control, Angle of attack.

NOMENCLATURE

STOL	Short takeoff and landing
CG	Center of Gravity
AC	Aerodynamic Center
Vh	Tail Volume Coefficient
lt	Tail moment arm
St	Tail surface area
$\underline{c}$	Mean chord
SA	Wing surface area
Cm,cg	Moment coefficient about the center of gravity
Clt	Coefficient of lift of the tail
$Cm0$	Moment coefficient at zero lift
α	Angle of attack
δe	Elevator deflection
it	Tail incidence angle

Cm	Moment coefficient
Cm,ac	Moment coefficient about the quarter chord
Cl	Coefficient of lift
hcg	Distance from datum point to plane center of gravity
hac	Distance from datum point to plane aerodynamic center
$\alpha trim$	Trimmed angle of attack
$\delta trim$	Elevator deflection at trim
ϵ	Downwash angle/ angle of air hitting the tail
$\bar{x}$	Average

INTRODUCTION

Short takeoff and landing (STOL) aircraft are crucial to Alaska due to the state's vast remote areas with limited length or no established runways. Bush aircraft, some of which are STOL capable, are used for transporting people and goods to and from remote locations such as hunting camps, cabins, and villages. While not always necessary, STOL aircraft allow bush pilots to land in shorter lengths when compared to a typical bush aircraft which allows for greater flexibility in landing locations. A lake that may be too small for a typical aircraft could be accessed by a STOL aircraft.

There is no exact definition of what makes an aircraft STOL. This being said, there are different levels of STOL aircraft. A Piper Super Cub is typically classified as a STOL aircraft with a takeoff distance of 200 ft, but the current STOL take off world record is only 11 ft [1]. The world record aircraft is also a Piper Super Cub, so what is the difference between a normal Piper Super Cub and the world record plane? There are a multitude of differences between the two aircraft, with the world record aircraft being highly modified with a more powerful powerplant, lighter materials, larger flaps, flow control devices, among other things. These modifications allow the aircraft to generate enough lift to take off much faster than the normal plane. Looking into each major modification, the larger powerplant allows the aircraft to accelerate to take off speed faster, and if the prop is oriented correctly, it can produce induced lift over the wings. A lighter plane means less lift is needed to be generated which correlates to lower ground speed and angle of attack (AOA) needed for takeoff and landing. Larger flaps and flow control devices work in conjunctions to make more lift through a higher effective angle of attack by changing the effective chord line through flap defection and keeping flow attached to the wing, minimizing stalling, through the flow control devices. It should be noted that optimizing aerodynamic performance is crucial and it is commonly achieved using wind tunnel experimentation and numerical simulation [2,3,4]

PROBLEM DEFINITION AND OBJECTIVES

Although they are necessary for high end STOL, larger flaps and wing flow control devices when at high angles of attack can envelop the tail in downwash making the plane lose tail authority resulting in a pitch down motion and not allowing the aircraft to achieve its highest

possible lift. A pitch down motion is not the most dangerous thing that can happen by losing tail authority. If the plane $\partial C_m / \partial \alpha$ is positive the plane will pitch up if tail authority is lost leading to a complete stall if control is not regained. This paper hopes to find modifications that can be made to certain STOL aircraft that will increase tail authority at high angles of attack while not significantly impacting other characteristics of the Aircraft. The aircraft modifications will not be restricted to the tail but can be implemented anywhere along the body. The main restrictions impacting the modifications that can be made are the weight of the modification, the drag created by the modification, the impact of the modification on the overall lift of the aircraft, and the constructability of the modification. The weight of the modification is critical in multiple facets. STOL aircraft are purposely built to be light to achieve a high lift to weight ratio so the plane can take off at lower speeds. Adding significant weight via modification would increase the total lift needed for takeoff meaning the plane would need to be on the ground longer to accelerate to the new higher needed takeoff speed. Making a modification that increases take-off distance is obviously against the spirit of STOL aircraft and will be avoided in this paper. Adding weight, specifically in the wrong areas, can impact the aircraft's center of gravity (CG). A shift in CG can either make an aircraft more or less stable depending on the CG's location and the location of the aerodynamic center (AC). Whether a shift forwards or backwards in CG will increase or decrease the stability is completely dependent on the specific aircraft and will need to be analyzed on a case-by-case basis. A large increase in drag, even if it did allow for much higher angles of attack, would increase take off distance due to more time being needed to reach takeoff speed due to more of the thrust force accelerating the aircraft being consumed by the drag force. Higher drag would also lead to less efficient cruise flights which, while irrelevant to the aircraft STOL capabilities, affect the aircraft's real-world use and would decrease their range. A decrease in overall lift, much like an increase in weight, would mean it would take longer for the plane to take off which, as established earlier, should be avoided in the design of modifications. A lot of STOL aircraft are either user modified from a separate plane or constructed from a kit. Meaning that it is typically the user who is working on the plane. This is why the constructability of the modification is important. It is likely that the user of the plane will be the one making the modification. Without access to high end fabrication equipment, the designed modification should be something that can be accomplished with the tools that were needed to assemble the aircraft or other common relatively inexpensive tools.

PROPOSED APPROACH

Modeled Aircraft

In order to properly analyze the stability and control of an aircraft it is necessary to simulate the airflow around the entire aircraft and not just the control surfaces. This is due to the fact that all surfaces on the aircraft are dependent on each other, and all affect each other in different ways. Because of this a model of the entire STOL aircraft must be used. The aircraft modeled for this analysis is a highly modified Piper Cub (A simple rag and tube fuselage with aluminum wings that are covered with fabric). This design has been modified to maximize its performance during STOL flights. These modifications include larger wings with leading edge slats and large single slotted semi-fowling flaps as well as an extremely high power to weight ratio power plant and extremely long travel suspension. The modified aircraft is pictured below in Figure 1.

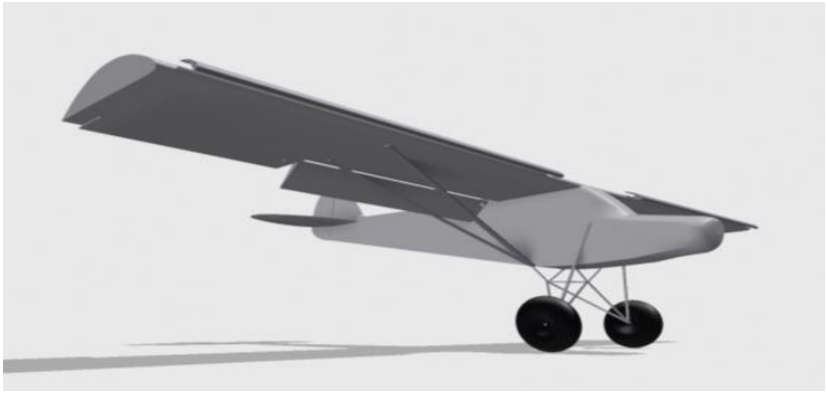

Figure 1: STOL Aircraft

The reason this aircraft is in need of a new tail design is the fact that with the addition of leading edge slats, large flaps, and an angle of incidence change, the aircraft can now operate at a much higher angle of attack than the original Piper Cub and thus the stock horizontal stabilizer and elevator are likely to be insufficient in maintaining authority over the pitch axis of the aircraft. The aircraft has an elevator deflection range of +-25^{o}. A horizontal stabilizer incidence range of 6 degrees. The range is +2^{o} up and -4^{o} down from wing incidence. The CG is 2 feet down (.3265 chord) and 2 feet behind (.3265 chord) the Leading edge or 0.6 feet down and 6.75 feet behind the prop hub. The weight of aircraft at this CG is 1400 lb. This aircraft has been 3D modeled to scale with a level of fidelity that balances simulation accuracy with simulation computation time in order to achieve the most efficient model for CFD analysis. The stock tail model is a horizontal stabilizer and a balanced elevator that are both flat plates as shown in modeled demonstrated in Figure 2.

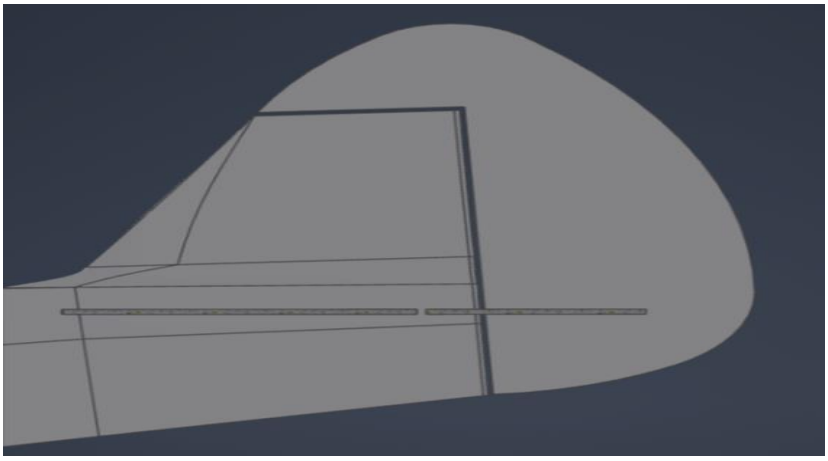

Figure 2: Stock Tail Design

The new tail design was determined based on qualitative and quantitative analysis of how the stock tail performed and found that the best method for our second iteration was to convert the horizontal stabilizer profile from a flat plate to an NACA 0009 airfoil in order to delay stall till a higher AOA and to enlarge the elevator to give greater control effectiveness. The new tail is shown in Figure 3.

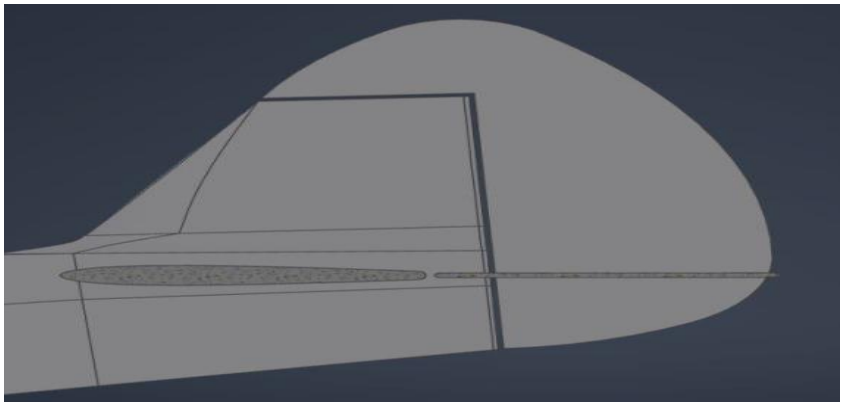

Figure 3: New Tail Design

Other new tail configurations were considered but rejected due to complexity and poor manufacturability.

CFD Preparations

To calculate the stability and control of the elevator, data for each design had to be gathered in multiple flight configurations. The three main parameters that were varied were elevator deflection angle, horizontal stabilizer incidence, and aircraft angle of attack. The most complete way to get data would be to run through every combination of these three variables with a 0.01-degree change. However, this is not a practical option given the time and computational constraints. It is also not completely necessary for the scope of this project. To keep computation time down, a set of 23 combinations was chosen to get relevant data. The following 20 combinations of these parameters were used to determine the high angle of attack performance. The list of configurations is shown in Table 1.

Table 1: List of Configurations

20deg AoA		**15deg AoA**	
Elevator deflection	**Stabilizer incidence**	**Elevator deflection**	**Stabilizer incidence**
15	-2	15	-2
10	-2	10	-2
5	-2	5	-2
0	-2	0	-2
-5	-2	-5	-2
-10	-2	-10	-2
-15	-2	-15	-2
0	2	0	2
0	0	0	0
0	-4	0	-4

In addition to these high angles of attack configurations, the elevator deflection and horizontal angle of incidence were fixed at 0°, and three configurations were made at 0° AoA, 5° AoA and 10° AoA. All of these configurations were chosen using the assumption that all behaviors will be linear (this is not an accurate assumption but is made for simplicity). Once the models were completed, the aircraft model was placed into Autodesk CFD 2026 and given an external air volume in the shape of a rectangular prism at a 10° angle to the nose of the aircraft with dimensions of (235.67, 222.2, 152.0) ft. This external volume size minimizes the chance that the boundary conditions will interfere with the actual flow near the aircraft. Once the external volume was created, material properties were applied to all parts. The external air volume was made with density equal to 1.20473 $\frac{kg}{m3}$, a temperature of 19.85°C and a viscosity of 1.817x10^-5 $\frac{kg}{ms}$. The aircraft was set to be made of aluminum as it has a similar roughness to the painted skin of the cub. After setting materials, boundary conditions were applied to the walls of the external air volume. All walls were given a component velocity boundary condition based on the angle of attack with the X velocity component being set to V_x = 30 cos (AoA-10deg) and the Z component being set to V_z = 30 sin (AoA-10deg). The faces of the external air volume were set to have a gauge pressure of 0 therefore equal to ambient air pressure. Once the boundary conditions were set, mesh sizing was set up. Auto sizing of the mesh was used with wall layers enabled with 10 layers, a layer factor of 0.45, and a layer gradation of 1.5. This allows for a fine mesh near the surface of the aircraft without creating a ridiculously large mesh where unnecessary which would significantly increase the calculation time and memory usage. These preparations were made for both configurations and for all selected tail configurations.

CFD Runs

After the simulations were prepared, they were exported to a higher power desktop computer with 64 GB of ram and a 12 core CPU for faster compute times. More ram and adequate cooling provided by the desktop configuration allowed for Autodesk CFD to be configured to run 3 simulations simultaneously, significantly cutting down on the needed compute time. All simulations were first run for 1000 iterations in steady state using the k-epsilon turbulence model. After completing 1000 iterations, or converging beforehand, 500 iterations of k-epsilon with intelligent wall formation were run until completion, or until convergence. Intelligent wall formation applies SST k-omega to the wall layers. SST k-omega is a more accurate turbulence model in the calculation of external aerodynamics and flow separation, both of which apply to the simulation being run [5]. The turbulence models k-epsilon and k-epsilon with intelligent wall formation were chosen due to their balance between computing time, reliability, and accuracy. Running k-epsilon without intelligent wall formation before any other turbulence models was a necessary step as it prevented the other models from diverging due to now having better starting values. K-epsilon, with intelligent wall formation was chosen over other turbulence models mainly because it offers low computation time in comparison to the other high accuracy models. K-epsilon with intelligent wall formation is less accurate than the other models, but the estimated total computing time to run both the 15° AOA and 20° AOA configurations, not accounting for down time, is roughly 2 weeks. Using a more computationally intense turbulence model could double or triple that compute time for just a small increase in accuracy which was not seen as necessary for this paper. Once each scenario had finished running, the whole file was exported with its results for analysis.

ANALYSIS AND DISCUSSION

From the CFD data, analysis was conducted to determine if the tail designs improved the stability and control in the pitch axis of the aircraft. The extracted data was used to compare the aerodynamic stability and the control performance of the stock tail and the new tail designs for the STOL aircraft, using the longitudinal-stability equations.

CFD Results

The CFD results were analyzed both qualitatively and quantitatively. Qualitative analysis was done by inspecting the flow velocities visually using cut planes such as in Figure 4 and Figure 5.

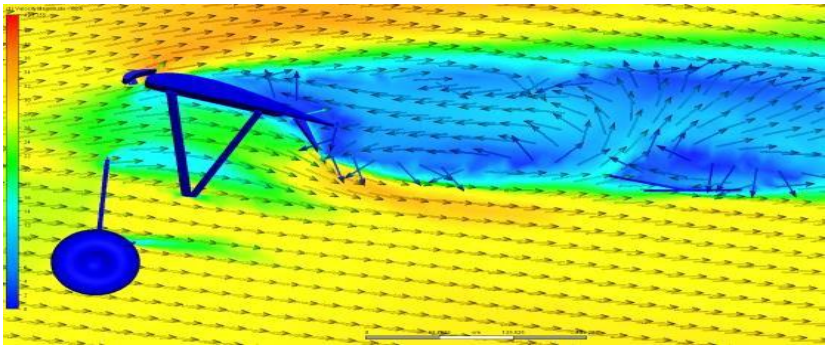

Figure 4: Stock Tail at 20° AoA

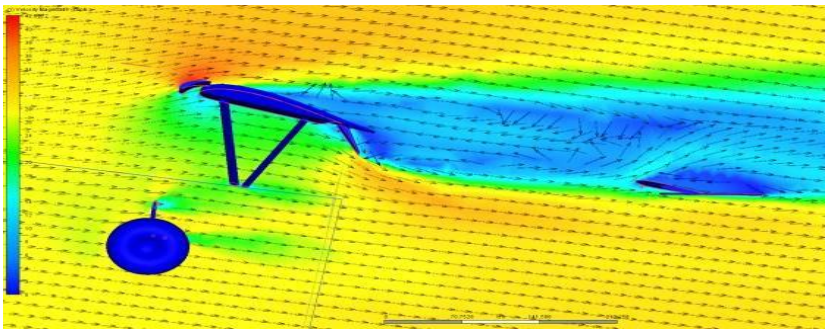

Figure 5: New Tail at 20° AoA

Multiple things can be deduced from comparing these two images. First, the flow separation on the wing was reduced from bringing the slats into the center of the wing. Second, a very close look at the bottom side of the elevator shows that on the stock tail there is stalling occurring. However, on the modified configuration, the stall on the bottom of the elevator has been eliminated. Similarly, it can also be inferred that the velocity of the air that is affecting the tail is more coherent and is not as turbulent and vortex filled. Values of quantitative analysis were extracted from all scenarios using a python script to calculate total forces and moments about the CG. This generated the raw data given in Appendix B.

Equations

Meanwhile, for both configurations considered, the following aerodynamic relationships are used to determine static stability and trim.

$$V_H = \frac{l_t S_t}{\bar{c} S_A} \quad \text{Eq. 1}$$

$$V_H = -\frac{C_{m,cg}}{C_{L_t}} \quad \text{Eq. 2}$$

$$C_{m0} = C_{m,cg} - \alpha\left(\frac{\partial C_{m,cg}}{\partial \alpha}\right) - \delta_e\left(\frac{\partial C_{m,cg}}{\partial \delta_e}\right) - i_t\left(\frac{\partial C_{m,cg}}{\partial i_t}\right) \quad \text{Eq. 3}$$

$$C_{m,ac} = C_{m,cg} - C_L(h_{cg} - h_{ac}) \quad \text{Eq. 4}$$

$$\alpha_{trim} = \frac{C_{m0}}{\frac{\partial C_{m,cg}}{\partial \alpha}} \quad \text{Eq. 5}$$

$$\delta_{trim} = \frac{C_{m0} + (\frac{\partial C_{m,cg}}{\partial \alpha})\alpha}{-\frac{\partial C_{m,cg}}{\partial \delta_e}} \quad \text{Eq. 6}$$

By picking two points from CFD data collection, we were able to find the slope from flow angles at two different absolute angles of attack (27.82° & 22.82°) (20° & 15°) geometric. The conversion between the absolute AOA and geometric AOA was calculated by taking the C_L at 0 geometric angle of attack and dividing it by the lift slope. The derivative $\partial\epsilon/\partial\alpha$ (downwash gradient) is what reduces the effective tail angle of attack and affects longitudinal stability. In the model, the downwash angle was found by finding the flow direction at a point just before the leading edge of the tail, located 11.18ft behind and 0.956ft above the airplane CG. The downwash gradient was then calculated by finding the change between the different modeled angles of attack. The average downwash gradient of all different configurations on the stock tail was found to be:

$$\bar{x}\left(\frac{\partial \varepsilon}{\partial \alpha}\right) = 0.887$$

And at the new tail

$$\bar{x}\left(\frac{\partial \varepsilon}{\partial \alpha}\right) = 1.845$$

While it would have been useful to use in certain equations, the calculated downwash gradients produce extraneous results possibly due to being located in an incorrect location where the stall vortex is affecting the direction of flow. Due to this, the calculated downwash gradients were ignored in all further calculations.

Tail Volume Coefficient and Static Stability

Using the geometry from our stock model:

$$l_t = 12 \text{ ft}$$

$$\bar{c} = 6.125 \text{ ft}$$

$$S_A = 202 \text{ ft}^2$$

$$S_t = 28 \text{ ft}^2$$

Where l_t is the tail moment arm, $\underline{c}$ is the mean chord length, S_A is the surface area of the wings, and S_t is the surface area of the tail. Plugging these values into Eq. 1 solves for the tail volume coefficient:

$$V_H \approx 0.272$$

This value is somewhat consistent with what was calculated from the CFD results using Eq. 2.

$$\bar{x}(V_H)stock = 0.2814$$

With the design of the new tail the only geometric value that changes is the tail surface area with the new value shown below:

$$S_t = 32.5 \text{ ft}^2$$

Plugging the new tail surface area into Eq. 1 yields the tail volume coefficient below:

$$V_H \approx 0.315$$

The tail volume for the new tail design is more closely consistent with what was obtained as an average from all the CFD data for configuration 2 and Eq. 2

$$\bar{x}(V_H)new = 0.345$$

From geometry the new tail therefore provides about 13.6% increase in tail-volume coefficient, and from the numerical calculation 18.4% increase in tail-volume coefficient giving it more authority over the pitch axis than stock. This higher V_h, results in a more negative slope $\partial C_{m/} \partial \sigma$, confirming greater static stability

Trim Behavior and Elevator Effectiveness

The trim equations (Eq. 3-Eq. 6) from above are used to find the equilibrium where Cm = 0. For the stock tail, higher elevator deflection is required to reach trim. It should be noted that for the new tail, trim occurs at a smaller elevator deflection, because the tail's larger surface area produces a stronger pitching moment. This is not surprising because the new airfoil horizontal stabilizer can achieve higher AOA without flow separation. The derivative $\partial C_{m/} \partial \delta_e$ becomes more negative for the new tail, which means the elevator generates more moment per degree of deflection. This improves our control response and could reduce the efforts in the inputs, which is valuable for STOL flight, where precise pitch control is critical.

Relationship between Geometric Angle of Attack and Elevator Deflection

The relationship between the geometric angle of attack (α) and elevator deflection (δ_e) provides some insight into elevator authority. For the stock tail shown in Figure 6, the trim

is approximately 12 degrees geometric AOA at zero elevator deflection and an approximate maximum achievable AOA of 22.5 degrees with full up elevator.

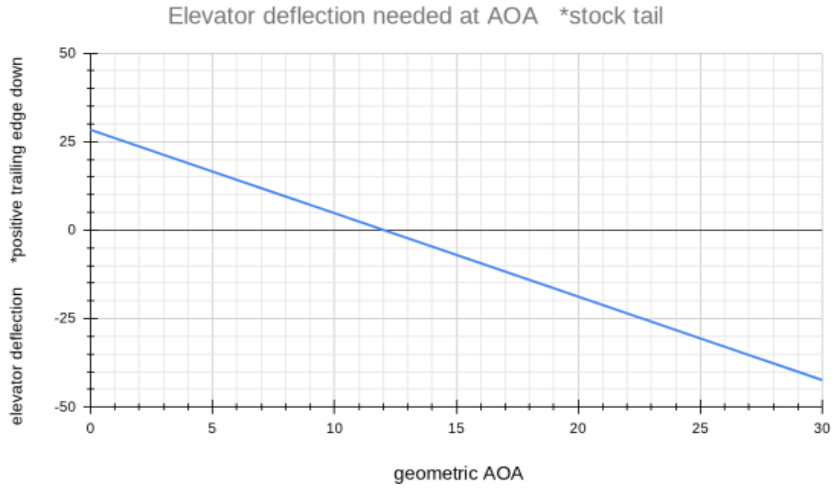

Figure 6: Elevator deflection needed at AOA (stock tail)

In the new tail shown in Figure 7, the trim is approximately 16 degrees geometric AOA at zero elevator deflection and an approximate maximum achievable AOA of 28 degrees with full up elevator. showing that the new tail has considerably more control strength over the stock tail.

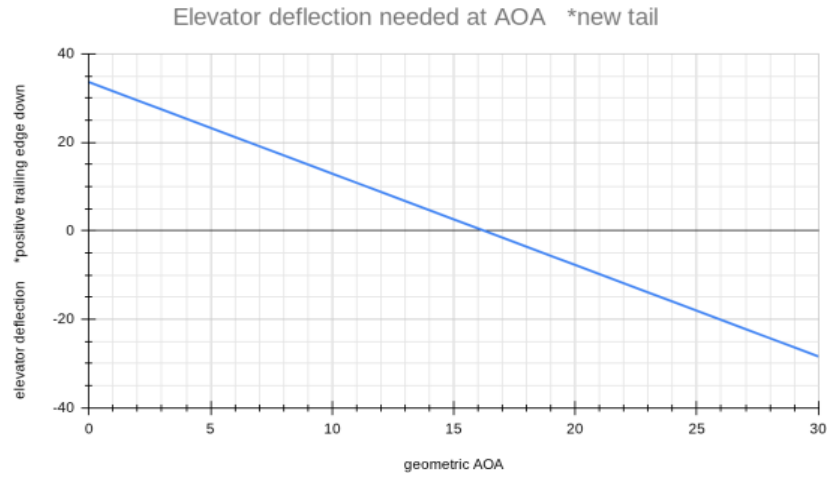

Figure 7: Elevator deflection needed at AOA (new tail)

The slope is steeper than with the stock tail, indicating greater control effectiveness. The stock tail requires a large elevator input, in order to achieve higher angles of attack. From Figure 6, an δ_e of +28.375° at AoA =0° and -18.799° at AoA =20° are needed to maintain trim meaning Cm,cg = 0. These two points give a slope of:

$$\frac{d\alpha}{d\delta e_{stock}} \approx -0.4239$$

From Figure 7, the new tail trims at δ_e = +33.596° at AoA = 0° and δ_e = -7.753° at AoA = 20°, giving a slope of:

$$\frac{d\alpha}{d\delta e_{new}} \approx -0.4836$$

This is about 12.3% improvement; it shows how the elevator produces more pitching moment per degree of deflection. Making the aircraft easier to control at high AoA and low speeds, which are some of the main requirements for STOL handling and overall pitch control.

CONCLUSION

Two separate tail designs for a highly modified STOL Piper Cub were constructed in CAD then exported into Autodesk CFD where multiple simulations were performed for varying angles of attack, incidence angles, and elevator deflections. The simulations were run with 1000 iterations of k-epsilon followed by 500 iterations of k-epsilon with intelligent wall formation which uses SST k-omega on wall layers. Once the simulations were run, a python script was used to extract the primary axial forces and torques on the aircraft from the simulation models. The stock and new tail designs were analyzed using simulation data along with geometric and aerodynamic parameters, the results of which are displayed in Table 2.

Table 2: Parameter comparison stock vs new

Parameter	Stock Tail	New Tail
Tail Volume (V_h)	0.317	0.368
Trim Elevator @ 0° AoA	+28.375°	+33.59°
Trim Elevator@ 20° AoA	-18.799°	-7.753°
Slope ($\frac{\partial \alpha}{\partial \delta_e}$)	-0.4239	-0.4836
controllability	Mild	Good

The new tail increases its tail-volume coefficient from 0.273 to 0.315, giving about 13.6% more stabilizing power. The trim elevator angles also improved. At 20° AoA it goes from -18.799° down to -7.753°, implied that the new tail has superior authority at higher angles of attack. The slope of the AoA–elevator curve was decreased from -0.4239 to -0.4836, which means the new tail has about 12.3% better elevator authority. The new tail gave stronger pitch stability and easier control at high angles of attack, which is very important for safe and effective STOL operation.

REFERENCES

[1] https://www.aopa.org/news-and-media/all-news/2018/may/17/valdez-stol-distances-get shorter

[2] S.F. Elsheltat, A.A. Alshara, W. Elshara, Aerodynamic evaluation of a symmetrical airfoil using wind tunnel testing, Afr. J. Adv. Pure Appl. Sci. 3 (4) (2024) 49–56. https://aaasjournals.com/index.php/ajapas/index.

[3] M. A. El Hady, A comparative study for different shapes of airfoils, J. Adv. Res. Fluid Mech. Therm. Sci. 69(1) (2020) 34–45, https://doi.org/10.37934/arfmts.69.1.3445.

[4] M. N. Kaya, A. R. Kök, H. Kurt, Comparison of aerodynamic performances of various airfoils from different airfoil families using CFD, Wind Struct. 32(3) (2021) 239–248, https://doi.org/10.12989/was.2021.32.3.239.

[5] https://help.autodesk.com/view/SCDSE/2024/ENU/?guid=GUID-E9E8ACA1-8D49-4A49-

APPENDIXES

Appendix A

Table 3: Model Parameters

conditions and characteristics	
Free stream velocity	44 ft/s
dynamic pressure (q)	2.300936 psf
wingspan (b)	36.67 ft.
density @ sea level	0.002377 slug/ft^3
wing chord (C)	6.125 ft.
wing area (S)	202 ft^2
New tail area(S_t)	32.5 ft^2
hcg	0.32653 c
hac	0.168367 c
wing leading edge to tail leading edge	14 ft.
lt	1.95918 c
V_h from geometry	0.367751

Table 4: Stock Tail Aerodynamic Coefficients

Stock tail	Averages
Cm,cg	-0.035
Cl	1.136
Cm,cgt	-0.074
Clt	0.276
Cm,ac	-0.214
Vh	0.2814
$Cm0$	0.16348

Table 5: Stock Tail Aerodynamic Derivatives

Stock tail	Averages
$\partial C_{m,cg}/\partial\alpha$	-0.0082347
$\partial C_{m,cg}/\partial\delta_e$	-0.0034912
$\partial C_{m,cg}/\partial i_t$	0.00220759
$\partial C_l/\partial\alpha$	0.0220853

$\partial C_{m,cgt}/\partial\alpha$	-0.0086175
$\partial C_{l_t}/\partial\alpha$	0.03
$\partial\epsilon/\partial\alpha$	0.887

Table 6: New Tail Aerodynamic Coefficients

New tail	Averages
Cm,cg	0.003
Cl	1.341
Cm,cg,t	-0.058
Clt	0.169
Cm,ac	-0.209
Vh	-0.342
$Cm0$	0.147

Table 7: New Tail Aerodynamic Derivatives

New tail	Averages
$\partial C_{m,cg}/\partial\alpha$	-0.009
$\partial C_{m,cg}/\partial\delta_e$	-0.004
$\partial C_{m,cg}/\partial i_t$	0.00002
$\partial C_l/\partial\alpha$	0.051
$\partial C_{m,cgt}/\partial\alpha$	-0.012
$\partial C_{l_t}/\partial\alpha$	0.035
$\partial\epsilon/\partial\alpha$	1.738

Appendix B

Table 8: Configuration 1 Raw Data

AoA(deg)	Elevator Incidence angle (deg)	tail Incidence (deg)	torque overall (lbf-ft)	lift overall (lbf)	tail torque (lbf-ft)	tail lift(lbf)
20	0	-2	-2.07E+02	5.76E+02	-3.32E+02	26.01705115
15	0	-2	-9.59E+01	5.17E+02	-2.14E+02	16.70433833
20	5	-2	-2.66E+02	5.78E+02	-3.91E+02	30.34723218
15	5	-2	-1.25E+02	5.17E+02	-2.51E+02	19.15185639
20	10	-2	-3.32E+02	5.87E+02	-4.57E+02	35.2382847
15	10	-2	-1.25E+02	6.36E+02	-2.80E+02	21.27498406

20	15	-2	-3.69E+02	5.93E+02	-3.98E+02	46.5845433
15	15	-2	-1.84E+02	6.16E+02	-2.73E+02	38.28701172
20	-5	-2	-1.25E+02	5.71E+02	-2.58E+02	19.93733229
15	-5	-2	-3.10E+01	5.04E+02	-1.62E+02	12.53791716
20	-10	-2	-5.02E+01	5.67E+02	-1.84E+02	14.62226303
15	-10	-2	5.52E+01	5.89E+02	-1.03E+02	7.998407472
20	-15	-2	2.37762135	5.58E+02	-1.33E+02	11.01721241
15	-15	-2	4.08E+01	4.90E+02	-9.59E+01	7.438936554
20	0	-4	-2.07E+02	5.78E+02	-3.32E+02	25.69340487
15	0	-4	-8.85E+01	5.22E+02	-2.14E+02	16.39880491
20	0	0	-1.77E+02	5.80E+02	-3.02E+02	23.68399908
15	0	0	-6.34E+01	5.26E+02	-1.99E+02	15.3956487
10	0	0	-1.48E+01	4.32E+02	-1.03E+02	8.166719722
5	0	0	1.11E+02	3.37E+02	7.38E+01	-5.521846334
0	0	0	2.26E+02	180.3038365	2.74E+02	-21.15561498
20	0	2	-1.84E+02	5.71E+02	-3.10E+02	24.0394401
15	0	2	-6.12E+01	5.19E+02	-1.84E+02	14.48358285

Table 9: Configuration 2 Raw Data

AoA (deg)	Elevator Incidence angle (deg)	tail Incidence angle (deg)	torque overall (lbf-ft)	lift overall (lbf)	tail torque (lbf-ft)	tail lift (lbf)
20	0	2	-5.97E+01	7.49E+02	-2.73E+02	21.31457967
15	0	2	4.82E+01	6.70E+02	-1.33E+02	10.06901751
20	0	0	-1.33E+02	7.22E+02	-3.39E+02	26.02542079
15	0	0	9.07E+01	6.86E+02	-1.03E+02	7.787417481
20	0	-2	-6.56E+01	6.47E+02	-2.43E+02	18.67483192
15	0	-2	5.10E+01	5.80E+02	-1.03E+02	7.8857939
20	0	-4	-5.97E+01	6.38E+02	-2.36E+02	17.97631889
15	0	-4	3.09E+01	5.46E+02	-1.11E+02	8.589841734
20	5	-2	-1.62E+02	7.37E+02	-3.69E+02	28.23346556
15	5	-2	4.41E+01	5.91E+02	-1.70E+02	13.15536857
20	10	-2	-2.29E+02	7.64E+02	-4.50E+02	34.0008348
15	10	-2	-4.94E+01	6.59E+02	-2.21E+02	16.55069711
20	15	-2	-2.80E+02	7.22E+02	-5.31E+02	40.69989571
15	15	-2	-1.03E+02	5.73E+02	-2.51E+02	18.77147956
20	-5	-2	-3.02E+01	7.10E+02	-2.43E+02	18.58720362

15	-5	-2	7.45E+01	5.78E+02	-8.11E+01	6.160184745
20	-10	-2	9.59E+01	7.26E+02	-1.25E+02	9.977016676
15	-10	-2	1.70E+02	5.78E+02	-4.72E+01	3.808702838
20	-15	-2	1.57E+02	7.08E+02	-6.12E+01	5.375668777
15	-15	-2	2.21E+02	6.59E+02	3.10E+01	-1.846796943
10.00	0.00	0.00	37.10	575.51	-95.88	7.27
5.00	0.00	0.00	132.76	348.45	120.96	-9.11
0.00	0.00	0.00	242.66	169.31	248.56	-18.77